Computer Methods in Biomechanics and Biomedical Engineering, 2015
Vol. 18, No. 12, 1272–1279, http://dx.doi.org/10.1080/10255842.2014.899587

Comparison of an EMG-based and a stress-based method to predict shoulder muscle forces

Christoph Engelhardt[a], Valérie Malfroy Camine[a], David Ingram[b], Philippe Müllhaupt[b], Alain Farron[c], Dominique Pioletti[a] and Alexandre Terrier[a]*

[a]*Laboratory of Biomechanical Orthopaedics, EPFL, Lausanne, Switzerland;* [b]*Automatic Control Laboratory, EPFL, Lausanne, Switzerland;* [c]*Orthopaedic and Traumatology Department, CHUV, Lausanne, Switzerland*

(*Received 9 July 2013; accepted 26 February 2014*)

The estimation of muscle forces in musculoskeletal shoulder models is still controversial. Two different methods are widely used to solve the indeterminacy of the system: electromyography (EMG)-based methods and stress-based methods. The goal of this work was to evaluate the influence of these two methods on the prediction of muscle forces, glenohumeral load and joint stability after total shoulder arthroplasty. An EMG-based and a stress-based method were implemented into the same musculoskeletal shoulder model. The model replicated the glenohumeral joint after total shoulder arthroplasty. It contained the scapula, the humerus, the joint prosthesis, the rotator cuff muscles supraspinatus, subscapularis and infraspinatus and the middle, anterior and posterior deltoid muscles. A movement of abduction was simulated in the plane of the scapula. The EMG-based method replicated muscular activity of experimentally measured EMG. The stress-based method minimised a cost function based on muscle stresses. We compared muscle forces, joint reaction force, articular contact pressure and translation of the humeral head. The stress-based method predicted a lower force of the rotator cuff muscles. This was partly counter-balanced by a higher force of the middle part of the deltoid muscle. As a consequence, the stress-based method predicted a lower joint load (16% reduced) and a higher superior–inferior translation of the humeral head (increased by 1.2 mm). The EMG-based method has the advantage of replicating the observed cocontraction of stabilising muscles of the rotator cuff. This method is, however, limited to available EMG measurements. The stress-based method has thus an advantage of flexibility, but may overestimate glenohumeral subluxation.

Keywords: shoulder; musculoskeletal model; muscle forces

1. Introduction

Knowledge about muscle forces exerted during movements is important to understand the functioning of joints as well as related orthopaedic conditions. The possibilities to measure muscle forces *in vivo* are limited. Non-invasive methods that measure joint movements or ground reactions forces only provide information on the forces exerted by groups of muscles. Invasive measurements are restricted to the use in operation rooms during surgeries, e.g. measurement of finger flexor muscle force (Dennerlein 2005). Minimal invasive methods can only be used on superficial tendons, e.g. the Achilles tendon (Finni et al. 1998). However, invasive approaches are in general not practicable in a clinical application. To overcome the experimental difficulties, several approaches exist to determine muscle forces theoretically. Two approaches are often found in musculoskeletal joint models: EMG-based methods and optimisation-based methods.

EMG-based methods use the experimentally measured electric muscle activation to estimate muscle forces through EMG data tracking (Erdemir et al. 2007). The advantage of EMG-based methods is to replicate as close as possible the muscular activity. However, the link between muscular activity and muscle force is still discussed and requires the use of muscle models with difficult to determine parameters. The main drawback of the method is the dependency on EMG data. This measurement is not only technically complicate, but requires the use of invasive fine wire electrodes for deep muscles. This method is therefore limited to the simulation of movements with available EMG and corresponding kinematic data.

In contrast, an optimisation-based method only needs kinematic input data. It minimises a cost function based on a physiological hypothesis. Different cost functions based on mechanical, energetic or metabolic hypothesis have already been proposed (Erdemir et al. 2007). The method requires an inverse dynamics approach to estimate the solution space for the simulated movement. Within this solution space, optimisation techniques are applied to minimise the cost function. The optimisation is usually constrained by further physiological criteria. Common constraints are the limitation of muscle forces to a maximum value, or joint stability criteria (van der Helm 1994b; Happee and Van Der Helm 1995). The main advantage of this method is its independence on EMG data. Its main drawback is the difficulty in correctly predicting the observed cocontraction of stabilising antagonist muscles (Cholewicki et al. 1995; Gagnon et al. 2001).

*Corresponding author. Email: alexandre.terrier@epfl.ch

EMG-based and optimisation-based methods have already been studied in several musculoskeletal joint models (Erdemir et al. 2007). In this work, we focused on the application of muscle force estimation methods on shoulder models. In the shoulder, the mechanical situation is different to other joints, as the shoulder is the only joint which is actively stabilised by muscles, the rotator cuff. Although several shoulder models exist using EMG-based (Langenderfer et al. 2005; Nikooyan et al. 2012) or optimisation-based (Karlsson and Peterson 1992; van der Helm 1994b; Buchanan and Shreeve 1996; Lin et al. 2004; Charlton and Johnson 2006) muscle force estimation methods, a direct comparison of the two methods within the same shoulder model could not be found. Furthermore, the existing EMG-based shoulder models do not include EMG measurements of the rotator cuff muscles, which, as stabilising muscles, are at risk to be underestimated by optimisation-based methods. Especially in stability analysis of the glenohumeral joint, the underestimation of rotator cuff muscle forces might lead to false conclusions.

Therefore, the goal of this work was to implement an EMG-based and an optimisation-based method within the same musculoskeletal shoulder model. The optimisation method minimises muscle stresses and is therefore referred to as the stress-based method in the following. The work was realised on a 3D model of the glenohumeral joint (Terrier et al. 2007, 2010, 2013), which is used to analyse issues related to total shoulder arthroplasty. The model has the ability to predict glenohumeral stability through the evaluation of humeral head translation. The resulting muscle forces, glenohumeral joint load and humeral head translations were compared.

2. Methods

2.1 Musculoskeletal shoulder model

The musculoskeletal shoulder model (Terrier et al. 2007) was based on cadaveric computer tomography (CT) scans of a shoulder without any sign of pathology. The model represented the glenohumeral joint after total shoulder arthroplasty (TSA). The glenohumeral joint was replaced by an Aequalis prosthesis (Tornier, Inc., Edina, MN, USA). The metallic humeral head sphere had a radius of 24 mm. The radius of the articular surface of the polyethylene glenoid implant was 30 mm. The model included the scapula, the humerus and 10 active muscle units: the subscapularis, supraspinatus, infraspinatus combined with teres minor, middle deltoid, anterior deltoid and posterior deltoid. The subscapularis and infraspinatus were each divided into three sections. The origins of the three sections were evenly distributed across the attachment zones on the scapula. The muscles were separated into a passive and an active part. The passive parts wrapped around the anatomic structure and the active parts generated the muscle force. Bones were assumed rigid. The humeral metallic component of the prosthesis was also assumed rigid. The glenoid implant was modelled as a linear elastic material with a Young's modulus of 500 MPa and a Poisson ratio of 0.4 (Kurtz et al. 2002). The articular contact between the glenoid implant and the humeral head sphere was assumed as a frictionless sliding contact.

We simulated a quasi-static movement of abduction in the scapula plane from a rest position to 150° of elevation. The Euler rotation angles of clavicle, scapula and humerus were implemented following an experimental study (McClure et al. 2001). The translation of the humeral head on the glenoid fossa was allowed. It was only constrained by the muscles, which wrapped around the bony structures. The moment arms of the muscles were continuously calculated during the movement accounting for humeral head translations. Sliding contacts were considered between muscles and bones. The arm weight was set to 3.75 kg (Damavandi et al. 2009).

The muscle forces must satisfy the mechanical equilibrium of moments:

$$\sum \mathbf{r}_m \times \mathbf{f}_m + \sum \mathbf{r}_e \times \mathbf{f}_e = 0, \qquad (1)$$

where $\mathbf{r}_m$ is the muscle moment arm, $\mathbf{f}_m$ the muscle force, $\mathbf{f}_e$ an external force and $\mathbf{r}_e$ the corresponding moment arm. Here, the arm weight was the only external force. The summation was done over the 10 muscle units. The left part of Equation (1) can be rewritten as

$$\sum \mathbf{r}_m \times \mathbf{f}_m = \mathbf{Rf} = \mathbf{q}, \qquad (2)$$

where $\mathbf{R}$ is the muscle moment arm matrix, the vector $\mathbf{f}$ contains the scalar values of all muscle forces and the vector $\mathbf{q}$ represents the resulting moment. The indeterminacy of the vectorial Equation (1) was solved by the EMG-based and stress-based methods.

2.2 EMG-based method

The EMG-based method solved the indeterminacy of the mechanical equilibrium with experimental EMG signals (Kronberg et al. 1990). The EMG measurements were obtained from five healthy volunteers in static positions every 30° of abduction. The EMG data were normalised to a voluntary maximum isometric contraction. To link muscle activation $\bar{a}_m$ and muscle force F_m, a Hill muscle model was implemented into the active muscle parts (Zajac 1989):

$$F_m = k\bar{a}_m f_m(l_m)\mathrm{PCSA}_m, \qquad (3)$$

where k is the Fick constant, $f_m(l_m)$ the isometric force–length relationship and PCSA_m the physiological cross-sectional area of the muscle. The activation $\bar{a}_m$ can vary between 0 (no activation) and 1 (maximum activation). The $f_m(l_m)$ and PCSA_m were taken from the literature (Langenderfer et al. 2004). In general, the experimentally measured muscle activities did not lead to muscle forces that fulfilled the mechanical equilibrium given in Equation (1). The following minimisation algorithm was implemented to estimate muscle activities a_m that stabilise the joint while remaining as close as possible to the experimentally measured activity $\bar{a}_m$:

$$\min\ G(a_m)\ \text{ with}: G(a_m) = \sum_{m=1}^{M} (a_m - \bar{a}_m)^2. \tag{4}$$

The minimisation problem was constrained by the mechanical equilibrium in Equation (1) and positive muscle activation:

$$0 < a_m < 1. \tag{5}$$

2.3 Stress-based method

The stress-based method used a pseudo-inverse null-space optimisation algorithm (Terrier et al. 2010; Ingram et al. 2012). The cost function g_1 was the sum of square muscle stresses.

$$\min\ g_1(\mathbf{f})\ \text{ with}: g_1(\mathbf{f}) = \sqrt{\frac{1}{n}\sum_{i=0}^{n}\left(\frac{f_i}{\mathrm{PCSA}_i}\right)^2}, \tag{6}$$

where PCSA_i is the cross-sectional area of the ith muscle. The optimisation problem was constrained by a physiological criterium. Muscles can only provide contractile forces, which were limited by a maximum value:

$$0 < f_i < f_i^{\max}(\mathrm{PCSA}_i, l_i). \tag{7}$$

This constrained indeterminate problem was solved in two steps. First, the cost function g_1 was minimised using Lagrange multipliers:

$$g_1(\mathbf{f}, \lambda) = \mathbf{f}^T\mathbf{E}\mathbf{f} - \lambda(\mathbf{R}\mathbf{f} - \mathbf{q}). \tag{8}$$

The matrix $\mathbf{E}$ was diagonal and contained the inverse of the values of the cross-sectional areas. The Lagrange optimisation led to the muscle forces $\mathbf{f}$. In a second step, we reduced the possible solution space to the physiological constraints from Equation (7). This was done by the optimisation of the null space $\mathbf{N}$ of the moment arm matrix $\mathbf{R}$:

$$\min\ g_2(\boldsymbol{\mu})\ \text{ with}: g_2(\boldsymbol{\mu}) = \frac{1}{2}\boldsymbol{\mu}^{\mathrm{T}}(\mathbf{N}^{\mathrm{T}}\mathbf{E}\mathbf{N})\boldsymbol{\mu} + (\mathbf{f}^T\mathbf{E}\mathbf{N})^T\boldsymbol{\mu}, \tag{9}$$

where $\boldsymbol{\mu}$ is a design parameter. The optimisation was constraint with

$$\begin{bmatrix} \mathbf{N} \\ -\mathbf{N} \end{bmatrix}\boldsymbol{\mu} \le \begin{bmatrix} f_1^{\max} - f_1 \\ \vdots \\ f_n^{\max} - f_n \end{bmatrix}. \tag{10}$$

Finally, the muscle force was

$$\mathbf{f} = \mathbf{R}^{+}\mathbf{q} + N\boldsymbol{\mu}. \tag{11}$$

2.4 Implementation

The musculoskeletal shoulder model and the two muscle force estimation methods were implemented in the finite element software Abaqus (Dassault Systèmes Simulia Corp., Providence, RI, USA). The implicit solver was used. The active contractile part of the muscle was modelled with a user-defined element (Terrier et al. 2007). This user-defined element included 2 nodes per muscle unit. The element was implemented in an Abaqus user element subroutine UEL. The subroutine was called by the implicit solver at each iteration of the Newton–Raphson algorithm. For both EMG-based and stress-based methods, the subroutine determined the contribution of the muscle element to the global stiffness matrix K^{MN} of the finite element method:

$$K^{MN} = -\frac{df^M}{du^N}, \tag{12}$$

where f^M is the contribution to the residual force vector and u^N are the nodal displacements of the user element. The nodal forces and the contribution to the global stiffness matrix were then returned to the solver.

The estimation of muscle forces with the EMG-based and stress-based method was implemented in the subroutine. The subroutine provided all variables required by both methods during the movement: the position of the arm, the lines of action and the moment arms of the muscles. The lines of action of the muscles were calculated using the displacement of the pair of points associated to each muscle (Terrier et al. 2007). The wrapping of the muscles around bony structures was taken into account in the line of action computation. The moment arm was determined by a cross product of two vectors. The first vector was defined from the centre of the humeral head to the muscle's insertion point. The second vector was defined from the muscle's insertion point into the direction of the line of action.

The EMG-based method required experimental muscle activations $\bar{a}$ for any elevation angle. The EMG data were interpolated with cubic splines. The interpolation was implemented in the Fortran subroutine by using the

PPPACK library (DeBoor 2001). The minimisation problem defined in Equation (4) was solved using the DQED library (Hanson 1986). The obtained muscle activities were then used to calculate muscle forces using Equation (3).

The stress-based method required a null-space algorithm of constrained quadratic programming. The pseudo-inverse of the moment arm matrix $\mathbf{R}^+$ in Equation (11) was obtained from the moment arm matrix. The LAPACK (Anderson et al. 1999) and BLAS (Blackford et al. 2001) libraries were used for all vector and matrix operations. The null space $\mathbf{N}$ was computed by a singular value decomposition. The algorithm was based on the divide and conquer approach. The constrained optimisation problem defined in Equation (9) was solved with the QPC solver included in the GALAHAD library (Gould et al. 2003).

3. Results

The forces of the rotator cuff muscles infraspinatus, suprascapularis and supraspinatus were significantly lower in the stress-based method compared with the EMG-based method (Figure 1(a)–(c)). At an abduction angle of 90°, the forces of infraspinatus were half the magnitude for the stress-based method compared with EMG-based method, respectively, at 60° for suprascapularis and supraspinatus. For both methods, the force of the middle deltoid increased during the elevation up to 80° and decreased afterwards (Figure 1(d)). For the stress-based method, the force of the middle deltoid was higher than in the EMG-based method during the whole movement. Maximum middle deltoid force was 18% higher for the stress-based method compared with the EMG-based method. In the stress-based method, posterior deltoid and anterior deltoid were inactive at the beginning of the abduction movement (Figure 1(e),(f)). The stress-based method predicted lower forces for the posterior deltoid and the anterior deltoid compared with the EMG-based method. In the EMG-based method, the predicted muscle activity for the rotator cuff muscles stayed close to the experimental data, with an average relative error of 11.3%. For the deltoid muscle, we observed an activation shift from the anterior to the posterior part, with an average relative error of 53.2%.

For both methods, the glenohumeral load (Figure 2(a)) increased during the elevation up to about 90° and

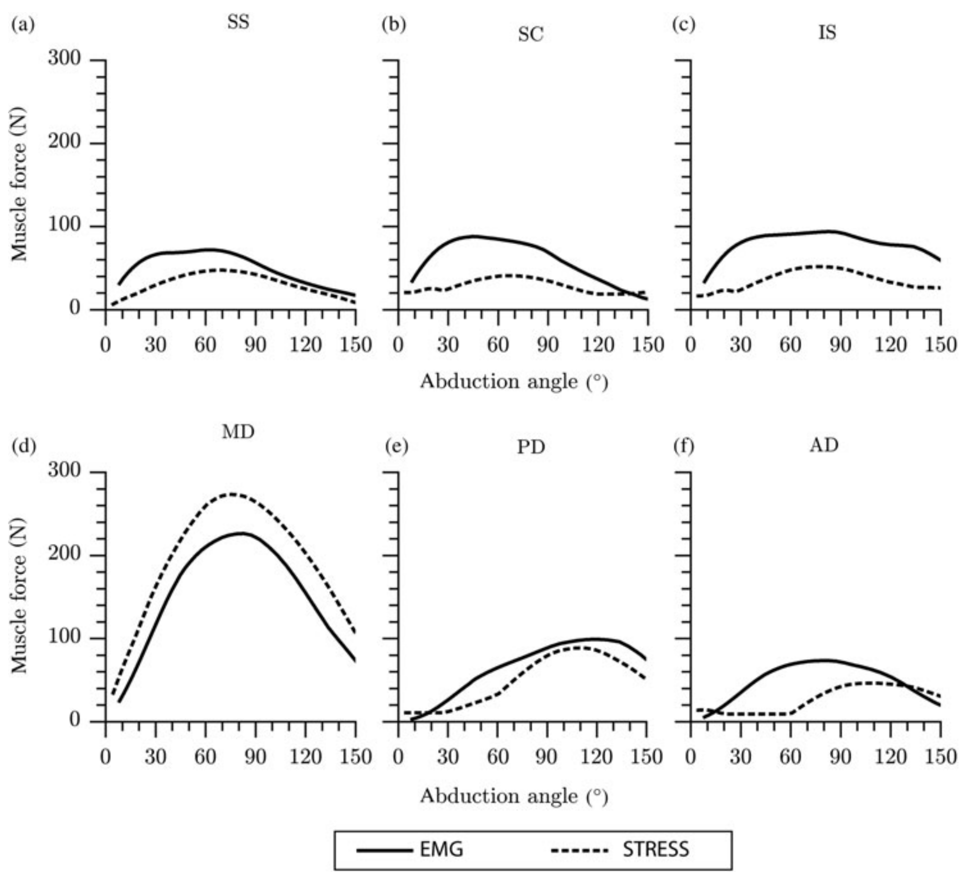

Figure 1. Predicted forces for rotator cuff muscles (a) supraspinatus (SS), (b) subscapularis (SC), (c) infraspinatus (IS) as well as (d) middle deltoid (MD), (e) posterior deltoid (PD) and (f) anterior deltoid (AD) during an abduction movement for the EMG-based and the stress-based methods.

decreased thereafter. Maximum values of 556 N corresponding to 65% BW (stress-based) and 478 N corresponding to 75% BW (EMG-based) were observed at 92° (stress-based) and 87° (EMG-based) abduction, respectively.

The stress-based method predicted a more eccentric articular contact than the EMG-based method. The contact area was 59 mm^2 for the stress-based method and 62 mm^2 for the EMG-based method at 90° abduction (Figure 3). The contact pressure reached 17 MPa with the stress-based method and 18 MPa with the EMG-based method.

In both methods, the humeral head was situated in a posterior position on the glenoid implant during the whole movement (Figure 2(b)). In both methods, we observed a translation from an initial inferior position to a superior position from 0° to 90° of abduction (Figure 2(c)). After 90° abduction, the humeral head descended again. For the stress-based method, the humeral head was in a more eccentric position throughout the whole movement compared with the EMG-based method.

4. Discussion

In this study, two widely used muscle force estimation methods were implemented and compared. The EMG-based method is using experimental EMG data as a reference. The stress-based method is using a constrained optimisation algorithm related to a stress-based cost function. Both methods were implemented within the same musculoskeletal shoulder model, to allow a direct comparison of muscle forces, joint loading and joint stability during an abduction movement. Both methods predicted the same tendencies, but the cocontraction of rotator cuff muscles was underestimated in the stress-based method. Their stabilising action was decreased compared with the EMG-based method.

The stress-based method resulted in reduced rotator cuff activity compared with the EMG-based method. While the EMG-based method followed the experimental data, the stress-based method tended to underestimate the force of muscles with small moment arms. In contrast, the middle deltoid, who had the largest moment arm, was favoured by the stress-based method. The middle deltoid was consequently more active in the stress-based method than in the EMG-based method. The anterior deltoid and the posterior deltoid were inactive at the beginning of abduction in the stress-based method. Below 60°, respectively, 30° elevation, their contraction would induce a counter-rotating moment. In contrast, the EMG-based method activated anterior and posterior deltoid during the whole movement, as prescribed by the EMG data. The underestimation of rotator cuff activity explained mainly the reduced joint loading in the stress-based method. Both models showed a superior–posterior migration of the humeral head during the abduction, but it was increased by the stress-based method compared with the EMG-based method. This was related to both reduced rotator cuff activity and higher middle deltoid force, which pulled the humeral head in the superior–posterior direction. Consequently, the articular contact was also situated in a more superior–posterior position in the stress-based method.

Our stress-based model predicted muscle forces comparable to the Delft shoulder model, but with lower amplitude. The middle deltoid force, for example, was half as big as in our model (van der Helm 1994). Conversely, our results showed different force patterns for the rotator cuff and deltoid muscles compared with the study of Yanagawa et al. (2008): infraspinatus and supraspinatus showed almost constant forces during the movement while our stress-based model predicted a maximum at 70° of abduction. Another study calculated muscle forces for glenohumeral abduction up to 80° glenohumeral elevation (Favre et al. 2012). Rotator cuff activity was higher compared with our stress-based method. Rotator cuff activity was not controlled by a cost function but a stability criterion. Most shoulder models predicted maximal joint

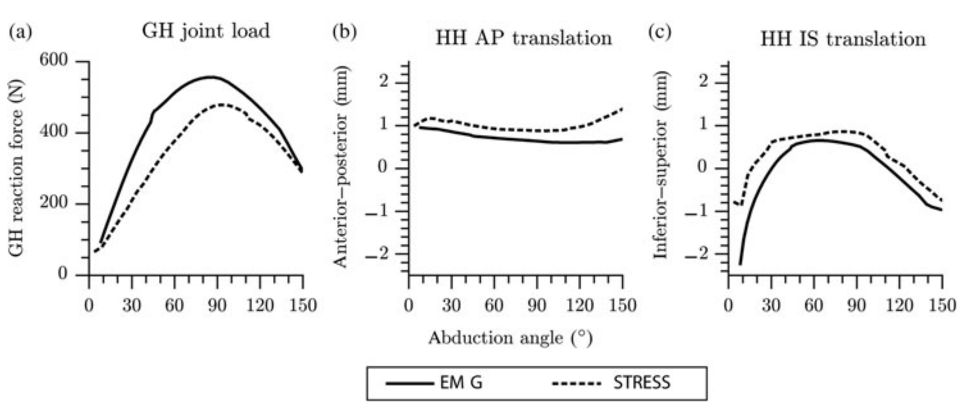

Figure 2. (a) Glenohumeral (GH) joint load, (b) anterior–posterior (HH AP) and (c) inferior–superior (HH IS) humeral head translations estimated with the EMG-based and the stress-based methods.

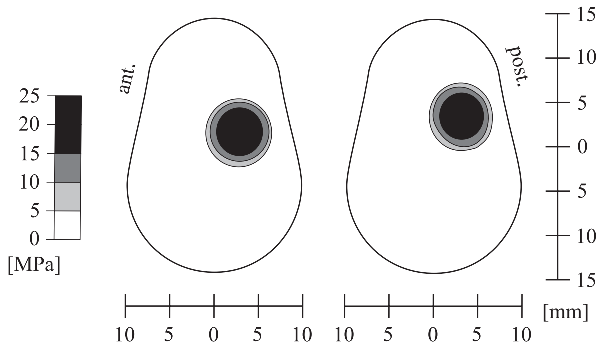

Figure 3. Glenohumeral contact pressure at 90° of abduction for the EMG-based (left) and the stress-based (right) methods.

reaction forces when the arm is in a horizontal position. In this position, the torque produced by the arm weight is maximal. The only other musculoskeletal model that considered humeral head translation (Favre et al. 2012) uncoupled humeral head translation from muscle force estimation. Although this model did not continuously update the muscle moment arms associated to humeral head translation, it predicted an upward migration of the humeral head followed by a descent in the second half of the abduction movement. The above reported differences between the numerical models can be explained by differences in underlying anatomic datasets, choice of represented muscles, modelling of muscles and the constraining of humeral head translations.

Several experimental *in vivo* studies measured the humeral head translation using radiography (Poppen and Walker 1976), open MRI (Graichen et al. 2000), CT fluoroscopy (Nishinaka et al. 2008) or MRI fluoroscopy techniques (Massimini et al. 2012). The studies reported an initial inferior position of the humeral head followed by an upward migration during the first phase of abduction and a downward displacement of the humeral head during the second phase of abduction (Poppen and Walker 1976; Graichen et al. 2000; Massimini et al. 2012). Only the study by Nishinaka et al. (2008) reported a continuous upward migration during the whole movement. For anterior–posterior translation, three studies (Poppen and Walker 1976; Graichen et al. 2000; Massimini et al. 2012) reported an initial anterior position followed by a posterior migration. After 90° abduction, the humeral head moved forward again (Poppen and Walker 1976; Graichen et al. 2000). Our numerical results are consistent with these *in vivo* measurements. The numerical prediction for glenohumeral joint force was in agreement with *in vivo* measurements for abduction angles under 90° elevation (Bergmann et al. 2011). Above 90° elevation, the experimental data showed a continuous increase while the numerical model predicted a decrease. However, abduction angles over 90° are rare in daily activity (Coley et al. 2008).

The strength of the present paper was to compare the stress-based and the EMG-based methods within the same musculoskeletal shoulder model. These methods have already been compared in other joints, and the lack of cocontraction in antagonist muscles has been reported. Thus, the novelty of this paper is that the underestimation of cocontraction in the stress-based method affected mainly the stabilising rotator cuff muscles. The present model allowed further the computation of humeral head translations for both methods and was thus able to show the tendency to subluxation in the stress-based method. The stability of the humeral head was naturally guaranteed through the compressive wrapping of the muscles. No additional stability criteria were implemented within the two methods proposed here, as it is done in other models (van der Helm 1994b; Favre et al. 2009; Engelhardt 2012).

The main limitation of the EMG-based method was the use of a Hill muscle model to link EMG measurements and muscle forces. The parameters of the Hill muscle model are difficult to quantify. However, the use of filtered, rectified and normalised EMG-data (Kronberg et al. 1990) is considered as a reasonable approach for use in static simulations (Lloyd and Besier 2003). Even if the study of Kronberg dates from 1990, it is still widely used. Furthermore, more recent studies that measure muscular activity of all shoulder muscles in static positions were not available. Then, the EMG data were not used to explicitly predict muscle forces, but rather to replicate patterns of muscular activity. The EMG data were measured on five healthy volunteers (Kronberg et al. 1990), but used in a model representing a shoulder joint after TSA. Nevertheless, anatomic prostheses are used in patients having regular muscular function. Muscular dysfunction would be an indication for an inverse prosthesis. The EMG-based method was then only compared with one constraint optimisation method using a stress-based cost function. The choice between force and stress-based cost functions seems, however, to have little influence on the results (van der Helm 1994b; Buchanan and Shreeve 1996). To reduce the degree of indeterminacy, only six muscles were included in the model. The deltoid muscles were included, as they are the main actors for the abduction movement, as well as the rotator cuff muscles, which are the main stabilisers of the glenohumeral joint. Including more muscles in the model would certainly influence the load distribution among the muscles. The use of an other anatomic data-set would also influence the computed muscle forces. Nevertheless, the discussed differences between EMG-based and stress-based methods would still be observable, as the differences rely on conceptional differences between the two methods.

In conclusion, both the EMG-based and the stress-based methods predicted muscle forces within the same range. For the analysis of forces, we would thus recommend the stress-based method because it requires less measured data. However, the stress-based method has limitations in the analysis of glenohumeral stability and tends to predict subluxation where there should not be any. For the analysis of load transfer and material stresses in implants and prosthesis, we would recommend the EMG-based method over the stress-based method as the latter predicts eccentric contact patterns. Several approaches exist to improve stress-based methods (Forster et al. 2004; Brown and Potvin 2005), but have not been used here as they require further physiological criteria or experimental data, thus removing one of the main advantages of the EMG-based method over the stress-based method. The possibility of direct comparison in the presented work might be helpful in further improving stress-based models by adjusting the activity of stabilising rotator cuff muscles.

Funding

This project was supported by the Swiss National Science Foundation [K-32K1_122512] and by the Inter-Institutional Centre for Translational Biomechanics [EPFL-CHUV-DAL].

References

Anderson E, Bai Z, Bischof C, Blackford S, Demmel J, Dongarra J, Croz JD, Greenbaum A, Hammarling S, McKenney A, et al. 1999. LAPACK users' guide. Philadelphia (PA): SIAM.

Bergmann G, Graichen F, Bender A, Rohlmann A, Halder A, Beier A, Westerhoff P. 2011. *In vivo* gleno-humeral joint loads during forward flexion and abduction. J Biomech. 44:1543–1552.

Blackford LS, Demmel J, Dongarra J, Duff I, Hammarling S, Henry G, Heroux M, Kaufman L, Lumsdaine A, Petitet A, et al. 2001. An updated set of basic linear algebra subprograms (blas). ACM Trans Math Software. 28:135–151.

Brown SH, Potvin JR. 2005. Constraining spine stability levels in an optimization model leads to the prediction of trunk muscle cocontraction and improved spine compression force estimates. J Biomech. 38(4):745–754.

Buchanan T, Shreeve D. 1996. An evaluation of optimization techniques for the prediction of muscle activation patterns during isometric tasks. J Biomech Eng. 118(4):565–574.

Charlton I, Johnson G. 2006. A model for the prediction of the forces at the glenohumeral joint. Proc Inst Mech Eng H. 220(8):801–812.

Cholewicki J, McGill SM, Norman. 1995. Comparison of muscle forces and joint load from an optimization and EMG assisted lumbar spine model: towards development of a hybrid approach. J Biomech. 28(3):321–331.

Coley B, Jolles B, Farron A, Aminian K. 2008. Arm position during daily activity. Gait Posture. 28(4):581–587.

Damavandi M, Farahpour N, Allard P. 2009. Determination of body segment masses and centers of mass using a force plate method in individuals of different morphology. Med Eng Phys. 31(9):1187–1194.

DeBoor C. 2001. A practical guide to splines. Rev. ed. New York: Springer. p. 346.

Dennerlein JT. 2005. Finger flexor tendon forces are a complex function of finger joint motions and fingertip forces. J Hand Ther. 18(2):120–127.

Engelhardt C, Ingram D, Müllhaupt P, Pralong E, Farron A, Pioletti D, Terrier A. 2012. Solving overconstrained kinematic in numerical shoulder model using nullspace optimization. 10th International Symposium CMBBE.

Erdemir A, McLean S, Herzog W, van den Bogert AJ. 2007. Model-based estimation of muscle forces exerted during movements. Clin Biomech. 22(2):131–154.

Favre P, Senteler M, Hipp J, Scherrer S, Gerber C, Snedeker J. 2012. An integrated model of active glenohumeral stability. J. Biomech. 45(13):2248–2255.

Favre P, Snedeker J, Gerber C. 2009. Numerical modelling of the shoulder for clinical applications. Philos Trans R Soc. 367:2095–2118.

Finni T, Komi PV, Lukkariniemi J. 1998. Achilles tendon loading during walking: application of a novel optic fiber technique. Eur J Appl Physiol Occup Physiol. 77 (3):289–291.

Forster E, Simon U, Augat P, Claes L. 2004. Extension of a state-of-the-art optimization criterion to predict co-contraction. J Biomech. 37(4):577–581.

Gagnon D, Larivière C, Loisel P. 2001. Comparative ability of EMG, optimization, and hybrid modelling approaches to predict trunk muscle forces and lumbar spine loading during dynamic sagittal plane lifting. Clin Biomech. 16(5):359–372.

Gould NIM, Orban D, Toint PL. 2003. Galahad, a library of thread-safe Fortran 90 packages for large-scale nonlinear optimization. ACM Trans Math Software. 29(4):353–372.

Graichen H, Stammberger T, Bonel H, Englmeier K-H, Reiser M, Eckstein F. 2000. Glenohumeral translation during active and passive elevation of the shoulder – a 3D open-MRI study. J Biomech. 33(5):609–613.

Hanson R. 1986. Linear least squares with bounds and linear constraints. SIAM J Sci Stat Comput. 7(3):826–834.

Happee R, Van Der Helm F. 1995. The control of shoulder muscles during goal directed movements, an inverse dynamic analysis. J Biomech. 28(10):1179–1191.

Ingram D, Müllhaupt P, Terrier A, Pralong E, Farron A. 2012. Dynamical biomechanical model of the shoulder for muscle-force estimation. 4th IEEE RAS/EMBS International Conference on Biomedical Robotics and Biomechatronics. New York: IEEE. pp. 407–412.

Karlsson D, Peterson B. 1992. Towards a model for force predictions in the human shoulder. J Biomech. 25 (2):189–199.

Kronberg M, Nemeth G, Brostrom L-A. 1990. Muscle activity and coordination in the normal shoulder. An electromyographic study. Clin Orthop Relat Res. 257:76–85.

Kurtz S, Villarraga M, Herr M, Bergström J, Rimnac C, Edidin A. 2002. Thermomechanical behavior of virgin and highly crosslinked ultra-high molecular weight polyethylene used in total joint replacements. Biomaterials. 23(17):3681–3697.

Langenderfer J, Jerabek S, Thangamani V, Kuhn J, Hughes R. 2004. Musculoskeletal parameters of muscles crossing the shoulder and elbow and the effect of sarcomere length sample size on estimation of optimal muscle length. Clin Biomech. 19:664–670.

Langenderfer JE, LaScalza S, Mell A, Carpenter JE, Kuhn JE, Hughes RE. 2005. An EMG-driven model of the upper extremity and estimation of long head biceps force. Comp Biol Med. 35(1):25–39.

Lin H-T, Su F-C, Wu H-W, An K-N. 2004. Muscle forces analysis in the shoulder mechanism during wheelchair propulsion. Proc Inst Mech Eng H. 218(4):213–221.

Lloyd DG, Besier TF. 2003. An EMG-driven musculoskeletal model to estimate muscle forces and knee joint moments in vivo. J Biomech. 36(6):765–776.

Massimini D, Boyer P, Papannagari R, Gill T, Warner J, Li G. 2012. *In vivo* glenohumeral translation and ligament elongation during abduction and abduction with internal and external rotation. J Orthop Surg Res. 7(1):1–9.

McClure P, Michener L, Sennett B, Karduna A. 2001. Direct 3-dimensional measurement of scapular kinematics during dynamic movements *in vivo*. J Shoulder Elbow Surg. 10:269–277.

Nikooyan A, Veeger H, Westerhoff P, Bolsterlee B, Graichen F, Bergmann G, van der Helm F. 2012. An EMG-driven musculoskeletal model of the shoulder. Hum Mov Sci. 31(2):429–447.

Nishinaka N, Tsutsui H, Mihara K, Suzuki K, Makiuchi D, Kon Y, Wright TW, Moser MW, Gamada K, Sugimoto H, et al. 2008. Determination of *in vivo* glenohumeral translation using fluoroscopy and shape-matching techniques. J Shoulder Elbow Surg. 17(2):319–322.

Poppen N, Walker P. 1976. Normal and abnormal motion of the shoulder. J Bone Joint Surg Am. 58(2):195–201.

Terrier A, Aeberhard M, Michellod Y, Müllhaupt P, Gillet D, Farron A, Pioletti D. 2010. A musculoskeletal shoulder model based on pseudo-inverse and nullspace optimization. Med Eng Phys. 32:1050–1056.

Terrier A, Larrea X, Camine VM, Pioletti D, Farron A. 2013. Importance of the subscapularis muscle after total shoulder arthroplasty. Clin Biomech. 28(2):146–150.

Terrier A, Reist A, Vogel A, Farron A. 2007. Effect of supraspinatus deficiency on humerus translation and glenohumeral contact force during abduction. Clin Biomech. 22(6):645–651.

Van der Helm F. 1994a. A finite element musculoskeletal model of the shoulder mechanism. J Biomech. 27(5):551–569.

Van Der Helm F. 1994b. Analysis of the kinematic and dynamic behavior of the shoulder mechanism. J Biomech. 27(5):527–550.

Yanagawa T, Goodwin C, Shelburne K, Giphart J, Torry M, Pandy M. 2008. Contributions of the individual muscles of the shoulder to glenohumeral joint stability during abduction. J Biomech Eng. 130(2):021024.

Zajac F. 1989. Muscle and tendon: properties, models, scaling, and application to biomechanics and motor control. Crit Rev Biomed Eng. 17(4):359–411.